

A Control Strategy for Hybrid Power Filter to Compensate Four-Wires Three-Phase Systems

Patricio Salmerón and Salvador P. Litrán

Abstract—A control algorithm is proposed for a three-phase hybrid power filter constituted by a series active filter and a shunt passive filter. The control strategy is based on the dual formulation of the compensation system principles. It is applied by considering a balanced and resistive load as ideal load, so that the voltage waveform injected by the active filter is able to compensate the reactive power, to eliminate harmonics of the load current and to balance asymmetrical loads. This strategy improves the passive filter compensation characteristics without depending on the system impedance, and avoiding the series/shunt resonance problems, since the set load-filter would present resistive behavior. An experimental prototype was developed and experimental results are presented.

Index Terms—Active power filters (APFs), harmonics, hybrid filters, instantaneous reactive power, power quality.

I. INTRODUCTION

MANY SOCIAL and economic activities depend on electrical energy quality and efficiency. Both industrial and commercial users are interested in guaranteeing the electrical waveform quality, which supplies their different systems. The nonlinear load can generate current harmonics and/or voltage harmonics, which makes worse the power quality. Therefore, these harmonics must be mitigating. In order to achieve this, series or parallel configurations or combinations of active and passive filters have been proposed depending on the application type [1], [2].

Traditionally, a passive LC power filter is used to eliminate current harmonics when it is connected in parallel with the load [3], [4]. This compensation equipment has some drawbacks [5] mainly related to the appearance of series or parallel resonances because of which the passive filter cannot provide a complete solution.

Since the beginning of the 1980s, active power filters (APFs) have become one of the most habitual compensation methods. A usual APF consists of a three-phase pulsewidth modulation (PWM) voltage source inverter. The APF can be connected either in parallel or in series with the load. The first one is especially appropriate for the mitigation of harmonics of the loads called harmonic current source. In contrast, the series configuration is suitable for the compensation of loads called

harmonic voltage source. The shunt connection APF is the most studied topology [6]–[10]. However, the costs of shunt active filters are relatively high for large-scale system and are difficult to use in high-voltage grids. In addition, their compensating performance is better in the harmonic current source load type than in the harmonic voltage source load type [10].

Another solution for the harmonic problem is to adopt a hybrid APF [11]–[18]. The hybrid topologies aim is to enhance the passive filter performance and power-rating reduction of the active filter. Two configurations have been mainly proposed: active filter connected in series with a shunt passive filter and series active filter combined with shunt passive filter. Both topologies are useful to compensate harmonic current source load type. However, when the load also generates voltage harmonics, the second topology is the most appropriate.

In this paper, the topology used is series active filter combined with shunt passive filter. For this configuration, different techniques have been applied to obtain the control signal for the APF [12]–[18]. The control target most used is that provides high impedance for the harmonics while providing zero impedance for the fundamental harmonic. This strategy is achieved when the APF generates a voltage proportional to the source current harmonics [12], [13]. With this control algorithm, the elimination of series and/or parallel resonances with the rest of the system is possible. The active filter can avoid that the passive filter becomes a harmonics drain of the close loads. Besides, it can prevent the compensation features from its dependence on the system impedance. From the theoretical point of view, the ideal situation would be that the proportionality constant k between the active filter output voltage and source current harmonics had a high value, at the limit it would be an infinite value. However, this would mean that the control objective was impossible to achieve. The chosen k value is usually small. It avoids high power active filters. However, the choice of the appropriate k value is an unsolved question, since it is related to the passive filter and the source impedance values. Besides, this strategy is not suitable to be used in systems with variable loads because the passive filter reactive power is constant, and therefore, the set compensation equipment and load has a variable power factor.

In another proposed control technique the APF generates a voltage waveform similar to the voltage harmonics at the load side, but in opposition [15]. This strategy only prevents the parallel passive filter depending on the source impedance; the other limitations of the passive filter nevertheless remain.

Other control strategies combining both the aforementioned have been proposed to improve the parallel passive filter compensation characteristics [11], but they go on suffering the difficulty of finding an appropriate value for the APF gain k .

Manuscript received August 5, 2009; revised November 9, 2009 and January 15, 2010. Date of current version June 18, 2010. Recommended for publication by Associate Editor P.-T. Cheng.

The authors are with the Electrical Engineering Department, Huelva University, Huelva 21819, Spain (e-mail: patricio@uhu.es).

Color versions of one or more of the figures in this paper are available online at <http://ieeexplore.ieee.org>.

Digital Object Identifier 10.1109/TPEL.2010.2043687

Finally, another approach has recently been proposed [16]. It suggests that the active filter generates a voltage, which compensates the passive filter and load reactive power, so it allows the current harmonics to be eliminated. The calculation algorithm is based on the instantaneous reactive power theory [19], [22]. There, the control target is to achieve constant power in the source side.

All presented strategies are applied to a three-phase three-wire system with balanced load.

In this paper, a control strategy based on the dual approach of the compensation principles is proposed, [21]. It is applied by considering a balanced and resistive load as ideal load. Thus, the determined reference voltage is obtained to attain the objective of achieving ideal behavior for the set hybrid filter load. With this strategy is possible to improve the passive filter compensation characteristics without depending on the system impedance, since the set load filter would present resistive behavior. It also avoids the danger that the passive filter behaves as a harmonic drain of close loads, and likewise, the risk of possible series and/or parallel resonances with the rest of the system. In addition, the compensation is also possible with variable loads, not affecting the possible the passive filter detuning. This strategy achieves unity power factor when the supply voltage is balanced sinusoidal. The system compensation can be applied to non-linear load, both harmonic current source loads and harmonic voltage source loads.

The control strategy was applied to a three-phase four-wire system. An experimental prototype was manufactured and its behavior checked. Experimental results are also presented.

II. REFERENCE COMPENSATION VOLTAGE

A. Proposed Control Strategy

Electrical companies try to generate electrical power with sinusoidal and balanced voltages and it has been obtained as a reference condition in the supply. Due to this fact, the compensation target is based on an ideal reference load, which must be resistive, balanced, and linear. It means that the source currents are collinear to the supply voltages and the system will have unity power factor. Therefore, at the point of common coupling (PCC), the following expression will be satisfied:

$$\mathbf{v} = R_e \mathbf{i}. \quad (1)$$

Here, R_e is the equivalent resistance, \mathbf{v} is the voltage vector on the connection point, and \mathbf{i} is the supply current vector.

Fig. 1 shows the configuration active filter connected in series with passive filter connected in shunt with the load.

In low voltage distribution systems, there is usually the presence of single-phase loads. That produces severe unbalance voltages and currents in the system. For this reason, even if the voltage source is balanced, the PCC voltage cannot be balanced due to the presence of unbalanced three-phase loads and/or single-phase loads. A compensating system will have to avoid the propagation of the voltage imbalance from the PCC to other consumers.

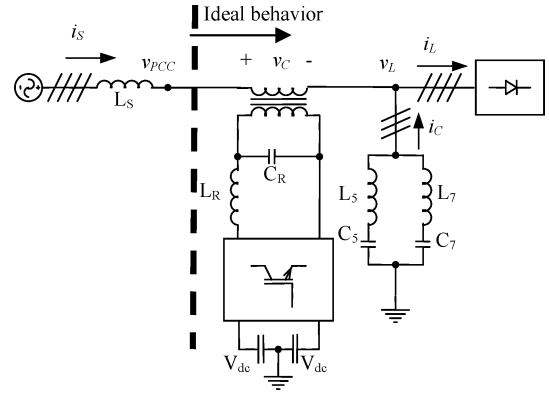


Fig. 1. Scheme of series active filter combined with shunt passive filter.

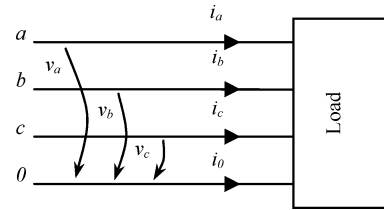


Fig. 2. Three-phase four-wire system.

In a three-phase system as in Fig. 2, the voltage and current vectors can be defined by

$$\mathbf{v} = [v_a \ v_b \ v_c]^T \quad \mathbf{i} = [i_a \ i_b \ i_c]^T. \quad (2)$$

When the load currents are unbalanced and nonsinusoidal, a balanced resistive load can be considered the ideal reference load. For the ideal load, the source current vector will be balanced and sinusoidal. The balanced current from (2) can be obtained applying the Fortescue transformation, defined by the following expression:

$$\begin{pmatrix} i^0 \\ i^+ \\ i^- \end{pmatrix} = \frac{1}{3} \begin{pmatrix} 1 & 1 & 1 \\ 1 & a & a^2 \\ 1 & a^2 & a \end{pmatrix} \begin{pmatrix} i_a \\ i_b \\ i_c \end{pmatrix}. \quad (3)$$

where $a = e^{j120}$ and zero-, positive-, and negative-sequence components are denoted by superscripts 0, +, and -, respectively.

The fundamental harmonic of the positive-sequence component i^+ , can be calculated applying the following relations:

$$\frac{1}{T} \int_0^T i^+ \sin \omega t \ dt = \frac{I_1^+ \sqrt{2}}{2} \cos \varphi \quad (4)$$

$$\frac{1}{T} \int_0^T i^+ \cos \omega t \ dt = \frac{I_1^+ \sqrt{2}}{2} \sin \varphi \quad (5)$$

where I_1^+ denote the rms value of the fundamental harmonic of i^+ , φ is its initial phase, and ω is the fundamental frequency.

The instantaneous value is given by the addition of (4) and (5), and multiplying (4) by $\sin \omega t$ and (5) by $\cos \omega t$, i.e.,

$$i_1^+ = I_1^+ \sqrt{2} (\cos \varphi \sin \omega t + \sin \varphi \cos \omega t). \quad (6)$$

With the inverse transformation, the ideal source current vector is obtained, which will be balanced and free of harmonics

$$\mathbf{i}_1^+ = \begin{pmatrix} i_{1a}^+ \\ i_{1b}^+ \\ i_{1c}^+ \end{pmatrix} = \begin{pmatrix} 1 & 1 & 1 \\ 1 & a^2 & a \\ 1 & a & a^2 \end{pmatrix} \begin{pmatrix} 0 \\ i_1^+ \\ 0 \end{pmatrix}. \quad (7)$$

The active power supplied by the source will be

$$P_S = I_1^{+2} R_e. \quad (8)$$

where I_1^{+2} is the norm of the positive-sequence fundamental component of the current vector [21], [22]. This norm is defined by

$$I_1^{+2} = \frac{1}{T} \int_0^T (\mathbf{i}_1^{+T} \mathbf{i}_1^+) dt. \quad (9)$$

The compensator instantaneous power is difference between the total real instantaneous power required by the load (p_L) and the instantaneous power supplied by the source (p_S), i.e.,

$$p_C = p_L - p_S. \quad (10)$$

When the average values are calculated in this equation and taking into account that the active power exchanged by the compensator has to be null, (10) can be rewritten as follows:

$$0 = \frac{1}{T} \int p_L dt - I_1^{+2} R_e. \quad (11)$$

Therefore, the equivalent resistance can be calculated by

$$R_e = \frac{1/T \int p_L dt}{I_1^{+2}} = \frac{P_L}{I_1^{+2}} \quad (12)$$

P_L is the load average power.

The aim is that the compensation equipment and load have ideal behavior from the PCC. The upstream voltage of the active filter can be calculated as follows:

$$v_{PCC} = \frac{P_L}{I_1^{+2}} \mathbf{i}. \quad (13)$$

where \mathbf{i} is the source current vector. Thus, the reference signal for the output voltage of the active filter is as follows:

$$\mathbf{v}_C^* = v_{PCC} - v_L = \frac{P_L}{I_1^{+2}} \mathbf{i} - v_L. \quad (14)$$

That is, when the active filter generates this compensation voltage, the set load and compensation equipment will behave as a resistor with a R_e value.

B. Comparison Between Resistive Load and Synchronous Reference Frame Methods

The synchronous reference frame (SRF) based control has been widely accepted by industrial sectors. Thus, some series active filter control schemes use techniques based on the SRF to extract the fundamental or harmonics component [24]. This method extracts the fundamental component without introducing any time delay at the steady state. However, this technique included generally a phase locked loop (PLL) in the detection system. It has good results when the current supply is balanced

TABLE I
CURRENT THD (%) FROM COMPARATIVE ANALYSIS OF THE TWO CONTROL METHODS

	Balanced			Unbalanced		
	Without Comp.	50Hz	49Hz	Without Comp.	50 Hz	49Hz
SRF	28.84	1.92	2.24	27.20	9.30	9.22
RL		1.31	2.20		2.26	3.07

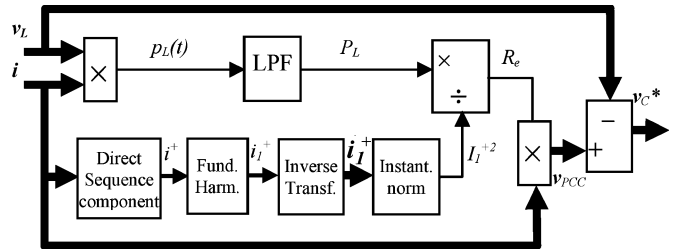


Fig. 3. Reference voltage calculation.

and includes low-order harmonics. The PLL usually has small bandwidth to reduce the effect of the high-frequency harmonics. This causes a poor dynamic response and an error in the detected magnitude. When the system is unbalanced, these errors affect to the fundamental component calculations.

In this section, a comparative analysis between proposed RL method and the SRF-based control is realized. The compensation system consists of combined filter constituted by an APF series and a parallel passive filter with two branch tuned to the fifth and seventh harmonics. Two control voltages have been implemented. One has been obtained by means of the proposed method in this paper; the other one has been obtained using the expression

$$v_{ch} = k i_{sh}. \quad (15)$$

where i_{sh} is the source current harmonics drawn from the utility. The current harmonics has been extracted using the SRF method.

Two nonlinear loads have been chosen: a balanced load and the another unbalanced load. Supply voltages with different frequencies 50 and 49 Hz, were applied to the loads. It was simulated with MATLAB-Simulink and total harmonic distortion (THD) results are presented in Table I. The SRF use a PLL to obtain the network frequency, however, the frequency in the RL method is fixed to 50 Hz in both cases.

The two techniques present a good behavior when a change in the frequency of the supply voltage takes place. When the load is balanced, the current THD are similar, however, when the load is unbalanced the SRF method present a current THD higher than the method RL proposed in this paper.

III. CONTROL SCHEME

A. Circuit Configuration

The control scheme used to calculate the active filter compensation voltage is shown in Fig. 3. It was implemented in MATLAB-Simulink. The toolbox real-time workshop (RTW) together with the real-time interface (RTI) from dSPACE

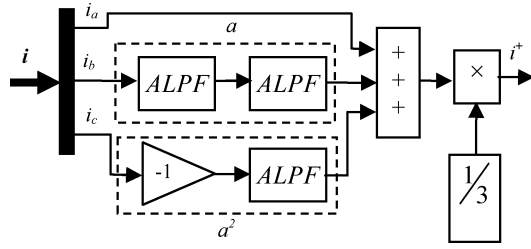


Fig. 4. Direct-sequence component calculation.

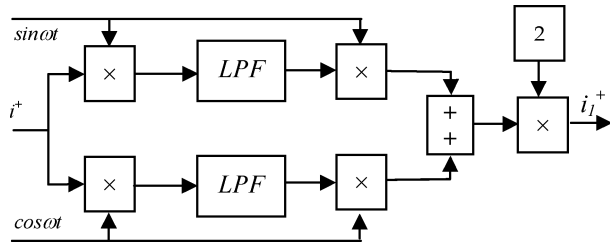


Fig. 5. Fundamental component calculation.

generates the code to program the control board. It let a rapid prototype of the control system presented and explained in Section IV.

The voltage vector at the load side and the source current vectors are the input signals. Fig. 8 shows the location of measurement sensors. The product of these vectors allows the instantaneous real power to be calculated, obtaining its average value with a low-pass filter (LPF). The LPFs are implemented with a Simulink block. This block is the model of a second-order filter, where the cutoff frequency was fixed to 100 Hz and the damping factor to 0.707. It let to reach a settling time of 8 ms.

The load average power P_L is divided by the norm of the current-positive-sequence fundamental component. For this, the positive-sequence component is calculated by means of the block “direct-sequence component,” where the Fortescue instantaneous transformation is applied. i.e.,

$$i^+ = \frac{1}{3} (i_a + ai_b + a^2i_c). \quad (16)$$

Here, the a operator is defined by

$$a = e^{j2\pi/3}. \quad (17)$$

It means a 120° phase shift. Fig. 4 shows the calculation scheme to determine the direct-sequence component. ALPF is an all-pass filter, implemented by means of Simulink transfer function block, it is defined by

$$F(s) = \frac{s - 181.4}{s + 181.4}. \quad (18)$$

The filter introduces a 60° delay at fundamental frequency, therefore, the a operator is achieved connecting two ALPF in cascade and a^2 inverting the input in the filter.

The fundamental component is obtained by means of a block with the scheme shown in Fig. 5. Each component of the source current vector is multiplied by $\sin \omega t$ and $\cos \omega t$, where ω is the fundamental frequency in radian/second. The average values of

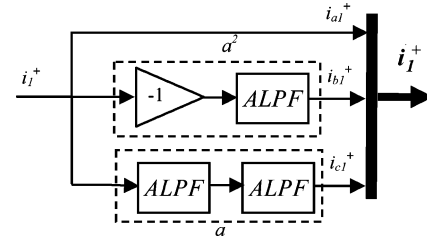


Fig. 6. Fortescue inverse transformation

the results are obtained using two LPFs. They are multiplied by $\sin \omega t$ and $\cos \omega t$ again, and then, by 2. This allows the fundamental harmonic of current direct-sequence component to be obtained.

The current fundamental component calculation could be affected when the source frequency changes. Simulations with MATLAB-Simulink for $\pm 2\%$ frequency variations have been performed. In the worse case, it makes an error in the calculation of a 0.01%. In addition, it is necessary to consider that IEC 50160 establishes that the frequency must remain within rank $50 \pm 1\%$. Therefore, any solution for the synchronization has not included. All the experimental results have been carried out with a 50 Hz source.

The Fortescue inverse transformation allows current vector of direct-sequence fundamental component to be obtained. It is calculated by means of

$$\vec{i}_1^+ = [i_{1a}^+ \ i_{1b}^+ \ i_{1c}^+]^T = [i_{1a}^+ \ a^2i_{1a}^+ \ ai_{1a}^+]^T. \quad (19)$$

which are the waveforms of the direct-sequence component of the current fundamental component. The calculation scheme is shown in Fig. 6.

The norm of the positive-sequence fundamental component of the current vector is defined by (9), however, when the current vector is sinusoidal and balanced, it can be calculated by the expression

$$I_1^{+2} = i_{1a}^{+2} + i_{1b}^{+2} + i_{1c}^{+2}. \quad (20)$$

Since i_{1a}^+ , i_{1b}^+ , and i_{1c}^+ have the same rms value and each phase shifted by an angle of 120° . This is implemented by the block “instant norm” in the Fig. 3.

The equivalent resistance is determined by the division between load average power and square norm of the positive-sequence fundamental component. The result is multiplied by the source current vector and the reference voltage is calculated, according to (14).

In the system, as shown in Fig. 8, there are two $2200 \mu\text{F}$ capacitors at the inverter dc side. The losses in the inverter can reduce and unbalance the capacitor voltages, therefore, the control scheme must include a loop with proportional-integral (PI) controller to ensure the capacitor voltages to remain constant [16] at the inverter dc side. Fig. 7 shows this control loop and the PWM generator. Here, V_{Ref} is the reference voltage to remain in the capacitors; $V_{\text{dc}+}$ and $V_{\text{dc}-}$ are the measured voltage. The difference between the reference value of the dc-link voltage and the monitored dc-link voltages serves as an input signal to the PI controller. The output controller is multiplied by

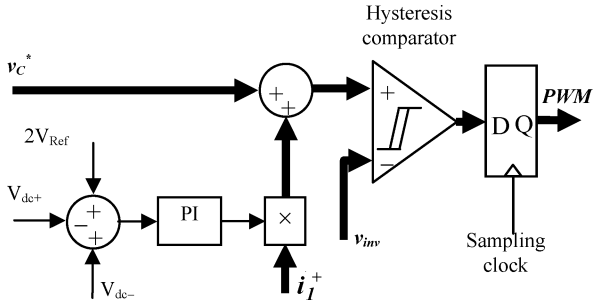


Fig. 7. Control dc-link and PWM generator scheme.

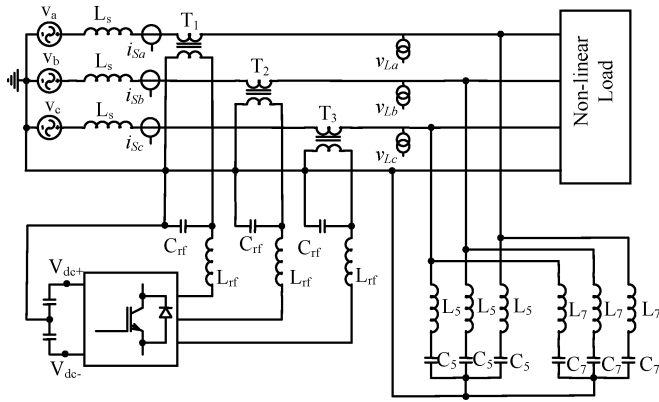


Fig. 8. Series APF and passive filter topology.

current direct-sequence fundamental component vector, which is added with the voltage v_c^* . It corrects the reference voltage calculated by means of (14). The modulation technique must be chosen according to the designed application. For APF use, the most important criterion could be a fast response, because the shape of the reference to be followed is very sharp in certain regions and very flat in other regions. On the other hand, it is very important to reduce high harmonics generated by the APF when it is designed to reduce the load distortion. For it, a hysteresis band control was developed. The insulated gate bipolar transistor (IGBT) gating signals are generated, comparing the reference signal with the inverter output voltage by considering a hysteresis band. This method switches the transistor when the error exceeds a fixed magnitude: the hysteresis band. Therefore, the switching frequency is variable, although in our design, this frequency is limited to 20 kHz, not to reach the IGBTs maximum switching frequency.

In Fig. 8(a) four-wire system is considered. In four-wire inverter, if the neutral conductor is connected to the dc bus midpoint, each leg can be controlled separately. This avoids that the current error can reach the double of the hysteresis band.

B. Stability Analysis

Fig. 9 shows an equivalent single-phase circuit of the system considering current and voltage harmonics. Here, V_S is the supply voltage, Z_S is the source impedance, Z_F is the passive filter impedance, and the nonlinear load is modeled by a current

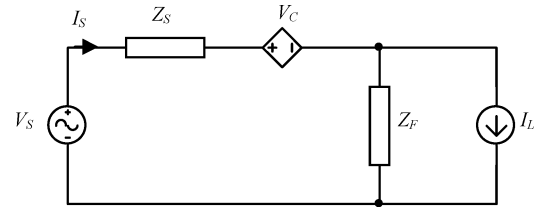


Fig. 9. Equivalent single-phase circuit.

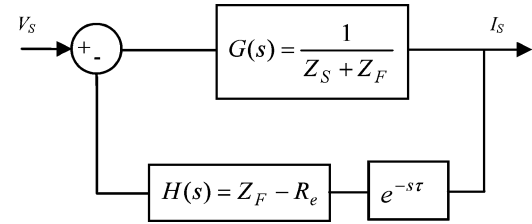


Fig. 10. Block diagram of the system.

source. In the equivalent circuit, the controlled voltage source represents the APF.

From the equivalent circuit, it is obtained

$$I_S = \frac{V_S + (Z_F - R_e) I_S}{Z_S + Z_F}. \quad (21)$$

With respect to the performance of the compensation, the system behaves like a closed-loop control system. Therefore, the analysis in the s domain could be developed with the help of the blocks diagram shown in Fig. 10. The transfer function $G(s)$ contains the impedances Z_F and Z_S , and the feedback block $H(s)$, includes the impedance Z_F and the equivalent resistance R_e , defined according to (12). For the sake of simplicity, the overall delay time of the control circuit τ is considered, thus the block with $e^{j s \tau}$ lets model the delay mainly due to the ALPFs.

The Nyquist criterion to analyze the stability of system is considered. Phase margin (Pm) is an effective index in addressing relative stability and dynamic performance. If the open-loop frequency response is relatively smooth in the gain/Pm region, the larger the Pm, the less the overshoot in the closed-loop step response. However, if $Pm < 0$, the closed-loop system is unstable. The open-loop transfer in Fig. 10 is given by

$$GH(s)e^{-s\tau}. \quad (22)$$

This criterion is applied to experimental prototype presented in Section IV. It is considered a $\tau = 50 \mu s$, which is the sample time in the control cards. It is possible to represent the equivalent resistance versus Pm, which let obtain the R_e values that do the stable system. Fig. 11 shows that the system is stable when $R_e < 62.1 \Omega$. Therefore, from the stability point of view, the experimental prototype is valid for these systems that fulfill this condition. In Section IV, the practical case corresponds to R_e values between 11 and 12 Ω . In the same Section IV appears the resulting waveform of a step change in the load.

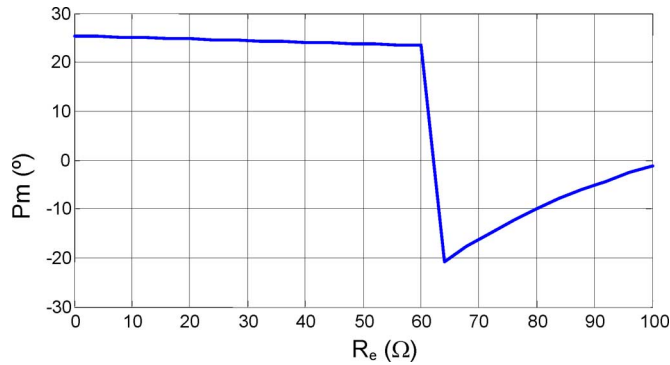


Fig. 11. Equivalent resistance versus Pm.

TABLE II
PASSIVE ELEMENT VALUES

Source	$L_s = 2.8 \text{ mH}; R_s = 1.8 \Omega$	
Passive filter	$L_5 = 13.5 \text{ mH}$	$C_5 = 30 \mu\text{F}$
	$L_7 = 6.75 \text{ mH}$	$C_7 = 30 \mu\text{F}$
Ripple filter	$L_{rf} = 13.5 \text{ mH}$	$C_{rf} = 50 \mu\text{F}$

IV. EXPERIMENTAL RESULTS

The experimental prototype has been developed. The power circuit is a three-phase system supplied by a sinusoidal balanced three-phase 100 V source and 50 Hz frequency with a source inductance of 2.8 mH and a source resistance of 1.8 Ω . The inverter consists of an IGBT three-legs bridge. It is a Semikron SKM50GB123-type IGBT bridge. Two 2200 μF capacitors are connected at the dc side. The reference voltage at the capacitors is 100 V. A small-rated passive filter LC has been included to eliminate the switching ripples at the inverter output. The selection criteria for ripple filter have been the following [13]: for low-frequency components, the inverter output voltage must be almost equal to voltage across C_{rf} . However, for high-frequency components, the dropped voltage in L_{rf} must be higher than in capacitor C_{rf} . Furthermore, L_{rf} and C_{rf} values must be selected to not exceed the transformer burden. Therefore, the following design criteria must be satisfied.

- 1) $X_{C_{rf}} \ll L_{C_{rf}}$, to ensure that inverter output voltage drops across L_{rf} at the switching frequency.
- 2) $X_{C_{rf}} \ll Z_S + Z_F$, to ensure that voltage divider is between L_{rf} and C_{rf} , where Z_S is the source impedance and Z_F is the shunt passive filter, reflected by the secondary winding.

At 20-kHz switching frequency, $Z_S = 728 \Omega$, $Z_F = 565 \Omega$, $X_{C_{rf}} = 0.16 \Omega$, and $X_{L_{rf}} = 1696 \Omega$. Table II includes their values.

The set inverter and ripple filter is matched to the power system by means of three single-phase transformers with a turn ratio of 1:1 to ensure galvanic isolation.

The passive filter is constituted by two LC branches tuned to the fifth and seventh harmonics; element values are included in Table II.

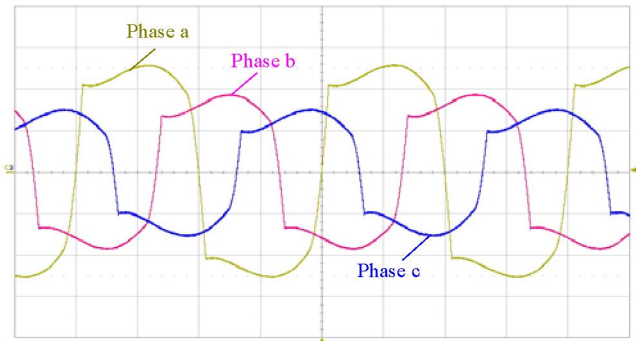


Fig. 12. Source currents, system without compensating 4 A/div. 5 ms/div.

The control strategy was implemented in a control and general application data acquisition cards compatible with MATLAB-Simulink and developed by dSPACE.

dSPACE RTI together with Mathworks RTW automatically generate real-time code. It allows the processor board to be programmed and I/O boards to be selected. It is based on the DS 1005 PPC placed in a dSPACE expansion box. The input board was the dSPACE DS 2004 A/D and the output board the DS 51001 DWO. The control board has a PowerPC 750GX processor running at 1 GHz. For developed experimental prototype, the sampling rate is limited to 50 μs in order to avoid overrun errors.

Shorts circuits in power distribution systems generate large currents that flow through the power lines, until the circuit breaker operates for clearing the fault. The power system equipment, such as power transformers, cables, buses, etc., are designed to withstand short circuit current during at least ten cycles, the series active filter may suffer severe damage during this short time. The withstand capability of the series APF depends mainly on the inverter power semiconductor characteristics. Therefore, a protection circuit must be included in the system. An interesting protection scheme is proposed in [25].

The nonlinear unbalanced load consists of three single-phase uncontrolled rectifiers with an inductor and a resistor connected in parallel at the dc side. The inductor is the same for the three phases 55 mH. However, the resistor was different for each phase; it was 8.3 Ω for phase *a*, 12.5 Ω for phase *b*, and 16.6 Ω for phase *c*. Fig. 12 shows the three source currents without compensation equipment. The currents are distorted and unbalanced. A three-phase power quality meters Fluke 434, was used to measure the THD, harmonics, and powers. The measured rms values for phase *a*, *b*, and *c* are 8.7, 6.1, and 5.0 A, and the current THD 28.5%, 27.6%, and 25.6%. The power factors are 0.91, 0.91, and 0.92 for each phase. Table III summarizes some measures.

The neutral current is shown in Fig. 13. The rms value is 5.4 A. The fundamental harmonic rms value is 3.3 A and the third harmonic is 4.1 A. They are most significant harmonics (see Table III).

Fig. 14 shows the source current in phase *a*, *b*, and *c* when the passive filter is connected. The rms values are similar to previous case, they are 8.6, 6.1, and 5.0 A. However, the THD values have risen to 34.9%, 32.4%, and 28.9%. Although the

TABLE III
MEASURED VALUE BEFORE AND AFTER THE COMPENSATION

		THD(%)	RMS	Fund.	H3	H5	H7	H9	P(kW)	Q(kvar)	S(kVA)	PF	S (kVA) APF	
Without compensation	Phase a	V	12.4	96	95.8	6.7	5.8	4.8	3.8	0.76	0.23 (ind)	0.79	0.91	-
		I	28.5	8.7	8.3	2	1.1	0.6	0.4					
	Phase b	V	9.1	97.1	96.7	4.4	3.9	3.6	3.1	0.54	0.17 (ind)	0.57	0.91	-
		I	27.6	6.1	5.9	1.3	0.7	0.5	0.3					
	Phase c	V	7.2	98.2	97.9	3.1	3.0	2.7	2.5	0.45	0.13 (ind)	0.47	0.92	-
		I	25.9	5.0	4.8	1.0	0.6	0.4	0.3					
Neutral		I	5.4	3.3	4.1	0.5	0.4	0.9	-	-	-	-	-	
With passive filter	Phase a	V	11.3	97.8	97.1	9.4	3.3	1.2	2.3	0.79	0.05 (ind)	0.79	0.93	-
		I	34.9	8.6	8.2	2.8	0.6	0.2	0.2					
	Phase b	V	7.6	98.9	98.6	6.1	2	0.6	1.6	0.57	0.02 (cap)	0.57	0.94	-
		I	32.4	6.1	5.8	1.8	0.4	0.1	0.2					
	Phase c	V	5.6	100	99.8	4.2	1.3	0.5	1.3	0.47	0.07 (cap)	0.78	0.94	-
		I	28.9	5.0	4.8	1.3	0.2	0.1	0.1					
Neutral		I	6.7	3.3	5.8	0.3	0.1	0.5	-	-	-	-	-	
With active and passive filter	Phase a	V	1.0	98.5	98.4	0.5	0.2	0.1	0.1	0.56	0.01	0.56	0.99	0.10
		I	2.6	5.7	5.7	0.1	0.0	0.0	0.0					
	Phase b	V	1.0	98.5	98.4	0.5	0.1	0.2	0.1	0.54	0.01	0.54	0.99	0.08
		I	2.6	5.5	5.5	0.1	0.0	0.0	0.0					
	Phase c	V	1.2	98.8	98.8	0.5	0.1	0.1	0.2	0.56	0.01	0.56	0.99	0.10
		I	2.9	5.7	5.7	0.1	0.0	0.0	0.0					
Neutral		I	0.5	0.3	0.4	0.0	0.0	0.0	-	-	-	-	-	

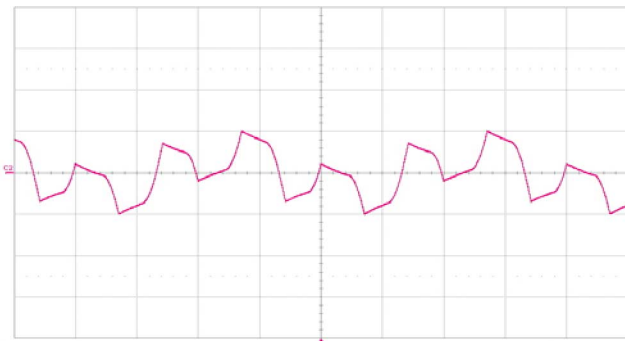


Fig. 13. Neutral current without compensating 10 A/div. 5 ms/div.

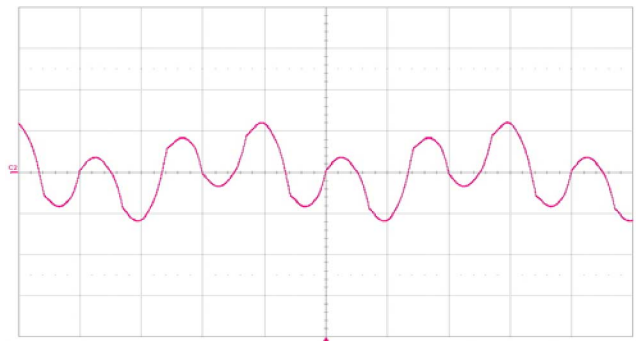


Fig. 15. Neutral current with passive filter 10 A/div. 5 ms/div.

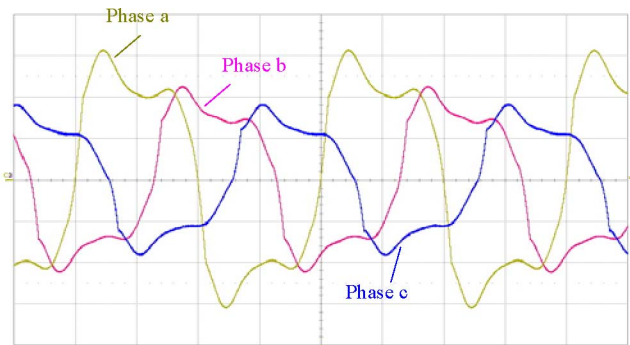


Fig. 14. Source currents, system with passive filter 4 A/div. 5 ms/div.

fifth and seventh harmonic is lower than previous situation, the third harmonic has gone up. It is due to the presence of this harmonic in the voltage at the PCC, which let to flow this component through the passive filter.

With the passive filter, the neutral current has 6.7 A rms value, being the fundamental component of 3.3 A, the same value that without passive filter and the third harmonic of 5.8 A. Fig. 15 shows the neutral current waveform.

Fig. 16 shows the source currents when the active filter is connected, then the source currents waveforms are sinusoidal and balanced, which is the aim of the control strategy. The power factor measured is practically the unit for the three phases. The rms values are 5.7, 5.6, and 5.7 A. There is a slight unbalance due to outliers in the measured sensors and modulation technique. The current THD are reduced to 2.6%, 2.6%, and 2.9%.

The neutral current is shown in Fig. 17. When active and passive filter are connected, the rms value is reduced to 0.5 A. The fundamental component is reduced to 0.3 A and the third harmonic to 0.4 A.

Fig. 18 shows the joint voltage and current of the *a* phase. They are practically sinusoidal and in phase. It demonstrates

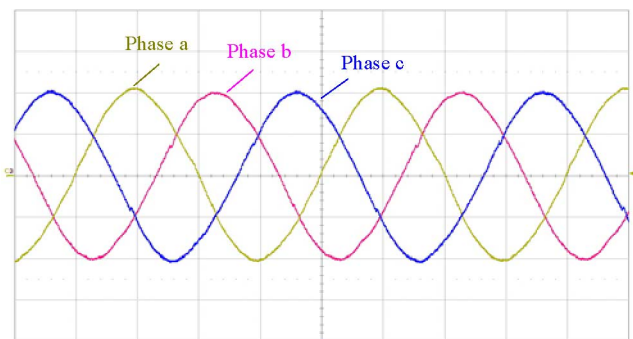


Fig. 16. Source currents, with passive and active filter 4 A/div. 5 ms/div.

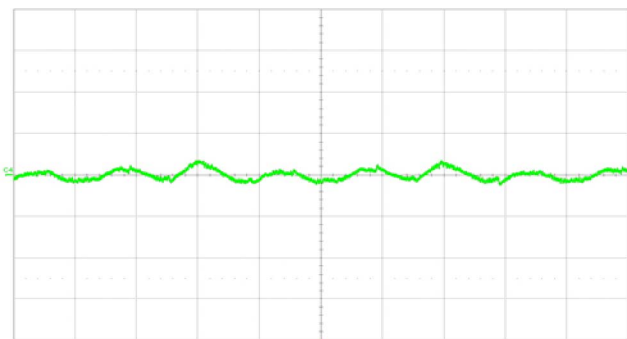


Fig. 17. Neutral current with passive and active filter 4 A/div. 5 ms/div.

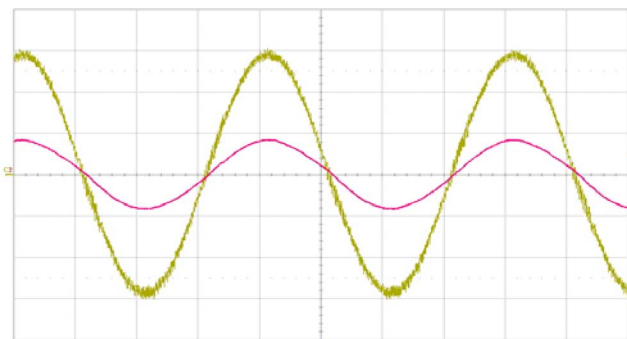


Fig. 18. Voltage and current at the PCC, *a* phase. Voltage 48 V/div and current 10 A/div. 5 ms/div.

the resistive behavior of the set compensation equipment load. Similar results are obtained to the *b* and *c* phase.

Table III summarizes the most important results. Harmonics, THD, powers, and power factors are included. The last columns show the active, reactive, apparent powers, and power factor per phase. The last column of Table III indicates the capacity of the APF series to obtain the harmonic filtering and the load balancing. An important part of the APF capacity is to correct load imbalance.

Finally, to verify the system dynamic response, a step change in the load has been experienced and the current waveform is recorded. Fig. 19 shows the response of the supply current when the resistance at the dc side of the single-phase rectifier connected in phase *c* changes from 16.6 to 9.1 Ω . When the full compensation equipment, active and passive filters, are

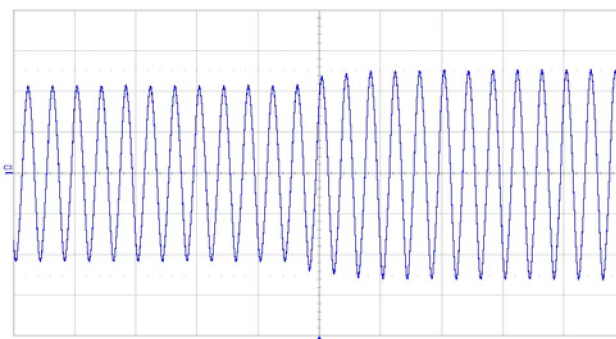


Fig. 19. Dynamic response of the source current of the compensated system 4 A/div. 50 ms/div.

connected to the system, the response time is about 3 cycles, what let verify the robustness of the control proposed in this condition.

The passive *LC* filters are unusually installed in low voltage, three-phase four-wire distribution system because *LC* filters tend to decrease the power factor, especially when the load have high distortion factor. This paper proposes a fifth and seventh tuned filter. Such design could leads to severe third harmonic voltage distortion because single-phase nonlinear loads produce significant third harmonic current. The resonance of the line impedance and the passive filters may be easily excited. As Table III shows, it is avoided with the active filter. When the active filter is offline due to malfunction or maintenance could appear this problem if the passive *LC* filter keeps online. The compensation equipment includes the active and passive filters; therefore, its disconnection is referred to the compensation system as a whole.

V. CONCLUSION

A novel control strategy based on the dual formulation of compensation system principles is proposed. It is applied by considering a balanced and resistive load as ideal load. Thus, the determined reference voltage is obtained to attain the objective of achieving ideal behavior for the set hybrid filter load. With this strategy is possible to improve the passive filter compensation characteristics without depending on the system impedance, since the set load filter would present resistive behavior. It also avoids the danger that the passive filter behaves as a harmonic drain of close loads, and likewise, the risk of possible series and/or parallel resonances with the rest of the system. In addition, the compensation is also possible with variable loads, not affecting the possible passive filter detuning.

The control strategy was applied to a three-phase four-wire system. An experimental prototype was manufactured and its behavior checked. Experimental results are also presented. It allows the verification of the developed theoretical analysis.

ACKNOWLEDGMENT

This paper has not been presented at a conference or submitted elsewhere previously. This work is part of the projects "A new technique to reduce the harmonic distortion in electrical

systems by means of equipment of active compensation," ref. DPI2004-03501, sponsored by the "Comisión Interministerial de Ciencia y Tecnología, CICYT, del Ministerio de Ciencia y Tecnología" of Spain, and "Design and implementation of a new equipment of active compensation with series connection for the improvement of the electrical waveform quality," ref. P06-TEP-02354, sponsored by the "Consejería de Innovación, Ciencia y Empresa de la Junta de Andalucía," of Andalucía, Spain.

REFERENCES

- [1] F. Z. Peng and D. J. Adams, "Harmonics sources and filtering approaches," in *Proc. Ind. Appl. Conf.*, vol. 1, Oct. 1999, pp. 448–455.
- [2] H. Akagi, "Active harmonic filters," *Proc. IEEE*, vol. 93, no. 12, pp. 2128–2141, Dec. 2005.
- [3] H. L. Ginn III and L. S. Czarnecki, "An optimization-based method for selection of resonant harmonic filter branch parameters," *IEEE Trans. Power Del.*, vol. 21, no. 3, pp. 1445–1451, Jul. 2006.
- [4] J. A. Pomilio and S. M. Deckmann, "Characterization and compensation of harmonics and reactive power of residential and commercial loads," *IEEE Trans. Power Del.*, vol. 22, no. 2, pp. 1049–1055, Apr. 2007.
- [5] J. C. Das, "Passive filters-potentialities and limitations," *IEEE Trans. Ind. Appl.*, vol. 40, no. 1, pp. 232–241, Jan. 2004.
- [6] P. Lohia, M. K. Mishra, K. Karthikeyan, and K. Vasudevan, "A minimally switched control algorithm for three-phase four-leg VSI topology to compensate unbalanced and nonlinear load," *IEEE Trans. Power Electron.*, vol. 23, no. 4, pp. 1935–1944, Jul. 2008.
- [7] B. S. Chen and G. Joos, "Direct power control of active filters with averaged switching frequency regulation," *IEEE Trans. Power Electron.*, vol. 23, no. 6, pp. 2729–2737, Nov. 2008.
- [8] F. Zhang and Y. Yan, "Selective harmonic elimination PWM control scheme on a three-phase four-leg voltage source inverter," *IEEE Trans. Power Electron.*, vol. 24, no. 7, pp. 1682–1689, Jul. 2009.
- [9] K. R. Uyyuru, M. K. Mishra, and A. Ghosh, "An optimization-based algorithm for shunt active filter under distorted supply voltages," *IEEE Trans. Power Electron.*, vol. 24, no. 5, pp. 1223–1232, May 2009.
- [10] T. A. Chaer, J.-P. Gaubert, L. Rambault, and M. Najjar, "Linear feedback control of a parallel active harmonic conditioner in power systems," *IEEE Trans. Power Electron.*, vol. 24, no. 3, pp. 641–653, Mar. 2009.
- [11] Z. Wang, Q. Wang, W. Yao, and J. Liu, "A series active power filter adopting hybrid control approach," *IEEE Trans. Power Electron.*, vol. 16, no. 3, pp. 301–310, May 2001.
- [12] F. Z. Peng, H. Akagi, and A. Nabae, "A novel harmonic power filter," in *Proc. IEEE/PESC*, Apr. 1988, pp. 1151–1159.
- [13] F. Z. Peng, H. Akagi, and A. Nabae, "A new approach to harmonic compensation in power systems—a combined system of shunt passive and series active filters," *IEEE Trans. Ind. Appl.*, vol. 26, no. 6, pp. 983–990, Nov./Dec. 1990.
- [14] A. Luo, Z. Shuai, W. Zhu, R. Fan, and C. Tu, "Development of hybrid active power filter based on the adaptive fuzzy dividing frequency-control method," *IEEE Trans. Power Del.*, vol. 24, no. 1, pp. 424–432, Jan. 2009.
- [15] G.-M. Lee, D.-C. Lee, and J.-K. Seok, "Control of series active power filters compensating for source voltage unbalance and current harmonics," *IEEE Trans. Ind. Electron.*, vol. 51, no. 1, pp. 132–139, Feb. 2004.
- [16] Y. S. Kim, J. S. Kim, and S. H. Ko, "Three-phase three-wire series active power filter, which compensates for harmonics and reactive power," *IEE Proc. Electr. Power Appl.*, vol. 151, no. 3, pp. 276–282, May 2004.
- [17] H. Yang and S. Ren, "A practical series-shunt hybrid active power filter based on fundamental magnetic potential self-balance," *IEEE Trans. Power Del.*, vol. 23, no. 4, pp. 2089–2096, Oct. 2008.
- [18] V. F. Corasaniti, M. B. Barbieri, P. L. Arnera, and M. I. Valla, "Hybrid active filter for reactive and harmonics compensation in a distribution network," *IEEE Trans. Ind. Electron.*, vol. 56, no. 3, pp. 670–677, Mar. 2009.
- [19] F. Z. Peng and J. S. Lai, "Generalized instantaneous reactive power theory for three phase power system," *IEEE Trans. Instrum. Meas.*, vol. 45, no. 1, pp. 293–297, Feb. 1996.
- [20] R. S. Herrera and P. Salmerón, "Instantaneous reactive power theory: A comparative evaluation of different formulations," *IEEE Trans. Power Del.*, vol. 22, no. 1, pp. 595–604, Jan. 2007.
- [21] P. Salmerón, R. S. Herrera, and J. R. Vázquez, "Mapping matrices against vectorial frame in the instantaneous reactive power compensation," *IET Electr. Power Appl.*, vol. 1, no. 5, pp. 727–736, Sep. 2007.
- [22] G. Superti-Furga and G. Todeschini, "Discussion on instantaneous p–q strategies for control of active filters," *IEEE Trans. Power Electron.*, vol. 23, no. 4, pp. 1945–1955, Jul. 2008.
- [23] S. Lee, J. Kang, and S. Sul, "A new phase detecting method for power conversion systems considering distorted conditions in power systems," in *Proc. IEEE Ind. Appl. Conf.*, 1999, vol. 4, pp. 2167–2172.
- [24] L. A. Moran, I. Pastorini, J. Dixon, and R. Wallace, "A fault protection scheme for series active power filters," *IEEE Trans. Power Electron.*, vol. 14, no. 5, pp. 928–938, Sep. 1999.



Patricio Salmerón was born in Huelva, Spain. He received the Ph.D. degree from the Electrical Engineering Department, University of Seville, Seville, Spain, in 1993.

In 1983, he joined Seville University as an Assistant, and then, became an Associate Professor in the Department of Electrical Engineering. Since 1993, he has been a Professor at Escuela Politécnica Superior, University of Huelva, Huelva, where he is currently a Dean. He was engaged in various projects, which includes research in power theory of nonsinusoidal

systems and power control in electrical systems. His research interests include electrical power theory, electrical power systems, active power filters, and power conversion systems.



Salvador P. Litrán was born in Sanlúcar de Barrameda, Spain. He received the B.Sc. degree in automation and industrial electronics engineering from the University of Seville, Seville, Spain, in 2002.

Since 1989, he has been teaching circuit theory and power electric system in the Department of Electrical Engineering, Escuela Politécnica Superior, University of Huelva, Huelva, Spain. His current research interests include power quality, electrical power theory, and active power filters.